Journal of
Instrumentation

Laboratory X-ray astrophysics at ultrabrilliant light sources with PolarX-EBIT

Published by IOP Publishing for Sissa Medialab

Received: *December 13, 2024*
Accepted: *February 17, 2025*
Published: *March 19, 2025*

The 15th International Symposium on Electron Beam Ion Sources and Traps
Kielce, Poland
27–30 August 2024

Laboratory X-ray astrophysics at ultrabrilliant light sources with PolarX-EBIT

S. Bernitt[a,b,c,d,*] **S. Kühn**[c] **M. Togawa**[c,e] **R. Steinbrügge**[f] **C. Shah**[g,c,h] **M.A. Leutenegger**[g] **P. Micke**[a,b,d] **Th. Stöhlker**[a,b,d] **and J.R. Crespo López-Urrutia**[c]

[a] *Helmholtz-Institut Jena, Fröbelstieg 3, 07743 Jena, Germany*
[b] *GSI Helmholtzzentrum für Schwerionenforschung GmbH, Planckstraße 1, 64291 Darmstadt, Germany*
[c] *Max-Planck-Institut für Kernphysik, Saupfercheckweg 1, 69117 Heidelberg, Germany*
[d] *Institut für Optik und Quantenelektronik, Friedrich-Schiller-Universität, Max-Wien-Platz 1, 07743 Jena, Germany*
[e] *European XFEL, Holzkoppel 4, 22869 Schenefeld, Germany*
[f] *Deutsches Elektronen-Synchrotron DESY, Notkestraße 85, 22607 Hamburg, Germany*
[g] *NASA/Goddard Space Flight Center, 8800 Greenbelt Road, Greenbelt, MD 20771, U.S.A.*
[h] *Department of Physics and Astronomy, Johns Hopkins University, Baltimore, Maryland 21218, U.S.A.*

E-mail: s.bernitt@hi-jena.gsi.de

Abstract: The x-ray spectra recorded with high-resolution spectrometers onboard satellite observatories contain valuable information about a wide range of different hot astrophysical environments. However, our ability to extract this information is currently often limited by the availability and accuracy of atomic data, as they are the foundation of plasma models. This is especially true for highly charged ions, ever-present in hot astrophysical plasmas. Laboratory x-ray spectroscopy experiments can provide the urgently needed data and benchmark atomic structure theories. PolarX-EBIT, a compact transportable electron beam ion trap based on permanent magnets, is used to provide targets of trapped highly charged ions for photon beams from ultrabrilliant synchrotron light sources. Resonant photoexcitation experiments have yielded atomic data for various highly charged ion species with unprecedented accuracy. Here, we provide a review of the capabilities of PolarX-EBIT, especially its transportability and off-axis electron gun, and the connected astrophysics-related research activities.

Keywords: Instrumentation for particle accelerators and storage rings - high energy (linear accelerators, synchrotrons); Plasma diagnostics - interferometry, spectroscopy and imaging; Ion sources (positive ions, negative ions, electron cyclotron resonance (ECR), electron beam (EBIS)); Instrumentation for FEL

*Corresponding author.

https://doi.org/10.1088/1748-0221/20/03/C03030

Contents

1 Introduction

Spectroscopic observations of the universe in the x-ray band with high-resolution spectrometers onboard satellite observatories like Chandra [1] and XMM-Newton [2] have contributed profoundly to our understanding of hot astrophysical plasmas. They have, among others, revealed compositions and states of stellar atmospheres [3], helped to model galaxy clusters [4, 5], and shown us details of winds outflowing from active galactic nuclei (AGN) [6, 7].

The next generation of non-dispersive x-ray spectrometers, based on microcalorimeters [8], has already been demonstrated to produce spectra of unprecedented quality during the short-lived Hitomi mission [9]. However, the potential for scientific discovery with missions like the X-ray Imaging and Spectroscopy Mission (XRISM) [10] and the proposed Athena [11] is currently limited by our understanding of atomic processes and spectroscopic features arising from them in hot plasmas [12–14]. There is a need for higher accuracy spectral databases and plasma models [15, 16]. Laboratory experiments with highly charged ions (HCI), ubiquitous in hot environments, are therefore necessary, to provide atomic data, as well as benchmark atomic structure theory.

Electron beam ion traps (EBITs) [17–19] use an electron beam, tightly focused by an external magnetic field, to ionize neutral atoms or ions in low positive charge states into higher positive charge states, by means of repeated electron impact ionization. The negative space charge of the electron beam also provides a radial trapping potential. Cylindrical drift tube electrodes around the beam axis provide an additional longitudinal trapping, resulting in three-dimensional confinement of the HCI. EBITs have proven to be versatile tools for spectroscopy on HCI, which are in such devices on average at rest in the laboratory frame and constantly excited by impact of electrons from the electron beam. This has enabled a wide range of laboratory measurements with spectrometers [20] and semiconductor detectors [21]. The electrons in the beam are nearly monoenergetic, with typical widths of the electron kinetic energy distribution on the order of 10 eV, as has been demonstrated with measurements of dielectronic recombination (DR) [22, 23]. It is also possible to study interactions of HCI with neutral gas directly inside the trap [24], or use an EBIT as a source of ions, as part of a larger setup [25, 26].

2025 JINST 20 C03030

2 Resonant photoexcitation with electron beam ion traps

The classical forms of spectroscopy, where either a dispersive element or an energy-sensitive detector are used to determine the energies of individual fluorescence photons, resulting in a histogram of energies, are often limited by the resolving powers of spectrometers and detectors. Additionally, fluorescence yields can be too low to make measurements feasible, or introduce systematic uncertainties caused by environmental instabilities over longer data-recording periods.

An alternative approach is resonant photoexcitation and detection of fluorescence as a function of the exciting-photon energy, also known as fluorescence laser spectroscopy [27]. This technique is widely used in many areas of physics and chemistry, but has been mostly limited to infrared, optical, and near-ultraviolet wavelengths. Resonant photoexcitation of electronic transitions in HCI, trapped inside an EBIT, has been demonstrated in the optical wavelength range [28], but also with monochromatized x-ray photon beams from ultrabrilliant free-electron laser and synchrotron light sources. A monochromatized photon beam is axially overlapped with the prolate cloud of trapped ions. The energy of photons in the beam is scanned over the range of interest and fluorescence is detected with one or more detectors mounted perpendicularly to the beam axis. Resonant absorption of photons from the beam and subsequent emission results in a corresponding increase in fluorescence observed. Pioneering works in this field have been conducted using the transportable FLASH-EBIT of the Max-Planck-Institut für Kernphysik (MPIK) in Heidelberg. Experiments were sucessfully conducted at the free-electron laser facilities FLASH (Free Electron LASer in Hamburg) [29] and LCLS (Linac Coherent Light Source) [30], as well as at the synchrotron light sources BESSY II (Berliner Elektronenspeicherring-Gesellschaft für Synchrotronstrahlung II) [31, 32] and PETRA III (Positron-Elektron-Tandem-Ring-Anlage III) [33–35].

FLASH-EBIT, like most EBITs used for spectroscopy experiments, employs a pair of superconducting magnet coils, reaching a flux density of 6 T at trap center. This requires cryogenic operation. The resulting size and complexity of the apparatus makes transport to and use at light source facilities challenging, and often completely prohibits experiments. Room-temperature EBITs with permanent magnets can reduce size and complexity, as well as cost. A class of such devices, the Heidelberg compact EBITs [23], was developed specifically with the requirements of resonant-photoexcitation experiments in mind, including transportability and high-numerical-aperture optical access, which allows detectors for radiation emitted by trapped ions to cover a larger solid angle, compared to most other EBITs. It uses a four-fold symmetric arrangement of permanent magnets, achieving 0.86 T magnetic flux density at the trap center. Development took place at MPIK, in collaboration with the University of Jena and the Physikalisch-Technische Bundesanstalt (PTB) in Braunschweig. One of the first implementations of this design was PolarX-EBIT, which became operational in 2016. A photograph of PolarX-EBIT is shown in figure 1.

In previous photoexcitation and photoionization experiments, the photon beams of synchrotrons or free-electron lasers were introduced through the electron collector and dumped onto the electron gun, either directly on or close to the cathode, which was necessary to keep the photon beams coaxially aligned with the electron beam, and therefore the cloud of trapped ions. This can result in damage to the cathode, or negatively impact trap operation by releasing photoelectrons or sputtered ions. These problems were addressed by equipping PolarX-EBIT with a novel off-axis electron gun [23], which allows the photon beam to propagate through it and the trap without being obstructed. The cathode is tilted by an angle of 22° with respect to the central trap axis. For aligning the beam with this axis, the

2025 JINST 20 C03030

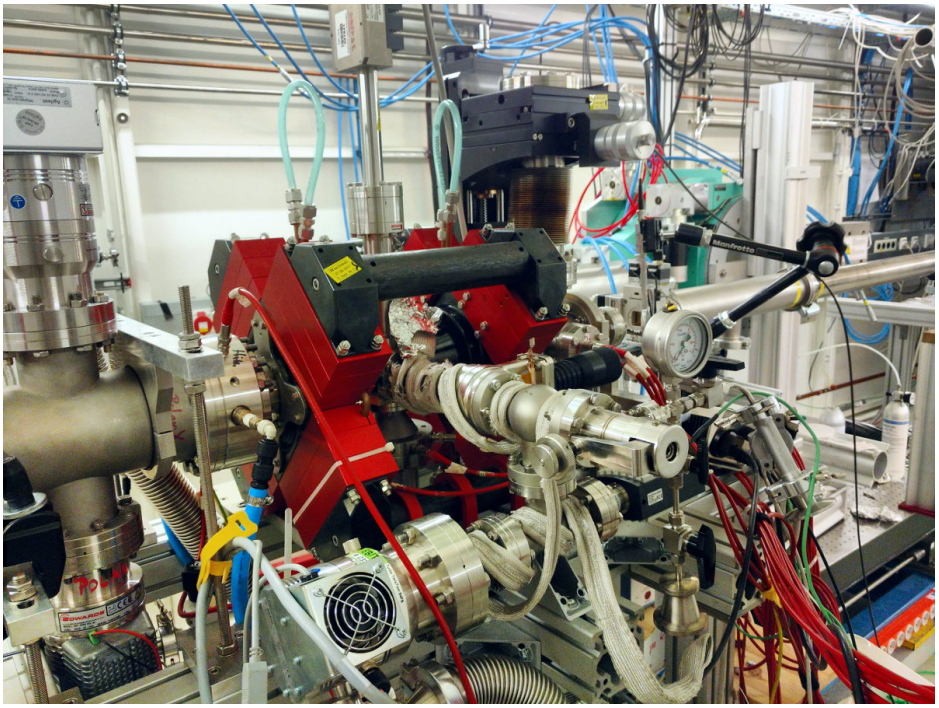

Figure 1. A photograph of PolarX-EBIT operating at beamline P01 of PETRA III. The monochromatized photon beam enters through the off-axis electron gun on the right and leaves unobstructed through the electron collector on the left. The red cartridges house 72 permanent magnets. The black parts connecting the cartridges are part of a soft iron structure used to guide the magnetic field. In the configuration shown, a window-less silicon-drift x-ray detector is mounted vertically on the top view port of the trap. Only the detector electronics are visible. The actual detector is mounted inside the vacuum chamber and located roughly 1 cm above the central drift tube.

anode is split into two separate electrodes by a cut at an angle of 35° (see figure 2). Electron currents of up to 30 mA and beam energies in the range from approximately 0.1 keV up to 8 keV have been achieved. While conventional on-axis electron gun setups can achieve significantly higher electron beam currents and energies, the ones achieved with PolarX-EBIT have proven to be by far sufficient for production and trapping of the mid-Z ions of interest for laboratory astrophysics. Additional protection for the cathode is provided by having the photon beam enter on the gun side and leave on the collector side, parallel to the electron beam, instead of anti-parallel, like in FLASH-EBIT. For photoexcitation cross-sections usually encountered in experiments with HCI, the ion cloud is largely transparent to the photon beam, which means that nearly all photons provided by the light source are not interacting inside the trap. The unobstructed beam can therefore leave PolarX-EBIT and be made available to downstream experimental setups. This ability, to be operated without blocking the beam, is a prerequisite to install an EBIT for longer periods of time as part of a radiation beamline at a synchrotron or free-electron laser facility. Typical pressures of 10^{-10} mbar to 10^{-8} mbar are compatible with the requirements of beamlines providing UV radiation or soft X-rays, where it is necessary to have a direct vacuum connection to allow transmission of radiation.

The device has been equipped with two silicon drift detectors, with active areas of 80 mm^2 and 150 mm^2, respectively. They are mounted perpendicularly to the trap axis and each other. One of them

2025 JINST 20 C03030

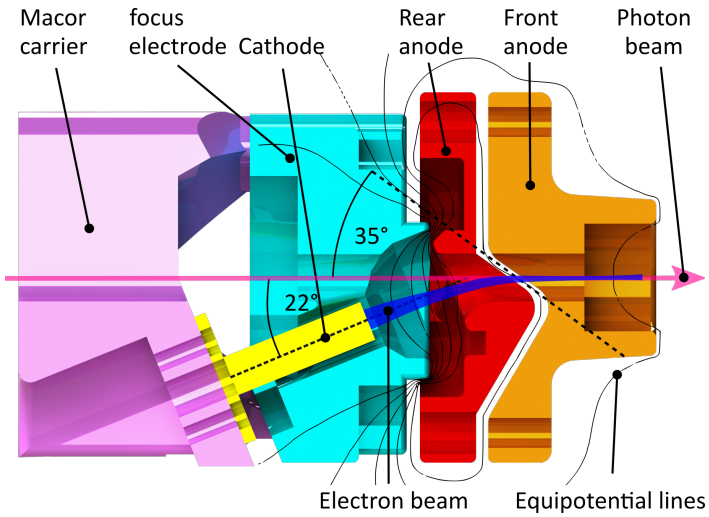

Figure 2. Cross-sectional view of the off-axis electron gun. The cathode (yellow) is mounted at an angle of 22° to the trap main axis, so that a photon beam (pink arrow) can pass through unobstructed. The anode is split into two parts (red and orange) and is used to bend the electron beam (blue) onto the trap main axis. The focus electrode (light blue) is also split into two parts, along the plane of the cross-section cut, to compensate the Lorentz force acting on the electrons in the magnetic field of the trap. Reproduced from [23]. CC BY 4.0.

is mounted horizontally and the other vertically. Visible light is blocked by filters made of 500 nm thick aluminium foil. As PolarX-EBIT is operated at room temperature, and the permanent magnet structure has been designed with access to the trap region in mind, the detectors can be operated close to the trap center, covering a solid angle of up to 1 sr. This is an improvement over typical operation at EBITs with cryogenic superconducting magnets, which requires detectors to be mounted farther away from the trapped ions. This arises from a need to minimize thermal radiation load for the cryogenic central trap region, as well as negative effects of strong magnetic fields on detectors and electronics. Both factors are not present in PolarX-EBIT, as there is no cryogenic system and the arrangement of permanent magnets with soft iron to guide the magnetic field [23] reduces field strength at the detector positions. Having two detectors, mounted at different angles, allows to observe the angular distributions of emitted fluorescence photons, when exitation is achieved with polarized light.

A typical width of the ion cloud is on the order of a few hundred µm. The widths of photon beams vary from light source to light source, but are usually of a similar size. Precise positioning of the EBIT is necessary to optimize overlap of ions and photons. For this purpose, it is mounted on three motorized feet. They allow vertical and horizontal translation perpendicular to the beam. In addition, pitch and yaw can be adjusted. After initial optical alignment and detection of resonantly excited fluorescence from known transitions, overlap is maximized based on fluorescence yield.

3 Experiments

As a transportable setup, PolarX-EBIT can be deployed at different ultrabrilliant light sources, opening up possibilities for a variety of experiments over a wide range of photon energies. As of now, experiments have been carried out at beamlines P01 and P04 of PETRA III, and at beamline U49-2/UGM-1 of BESSY II. An overview of the main components of typical experimental setups is shown in figure 3.

2025 JINST 20 C03030

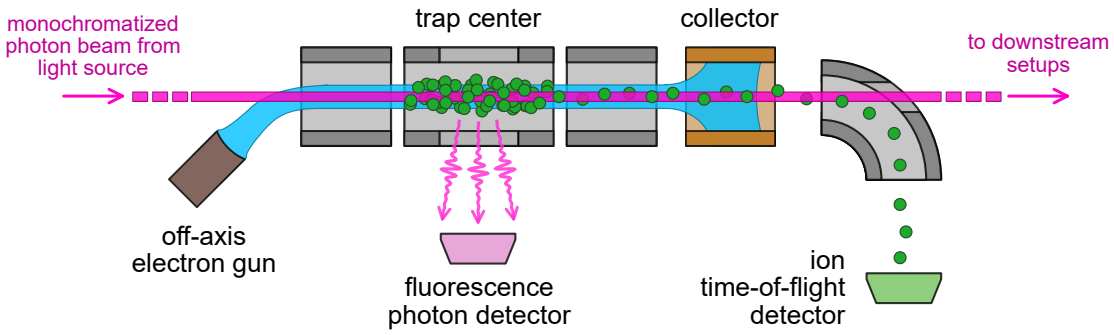

Figure 3. Main components of a typical experimental setup with PolarX-EBIT. The electron beam is shown in blue. Ions are shown in green. A monochromatized photon beam is provided by an ultrabrilliant light source and enters the trap through the central bore of the off-axis electron gun. Resonantly excited fluorescence is detected by one or more detectors (light pink) mounted perpendicular to the beam axis. If necessary, the ion charge state distribution can be measured via ion time-of-flight, after emptying the trap and guiding ions onto a channeltron (light green). The largely unabsorbed photon beam leaves the trap through the electron collector and is made available to downstream experiments.

3.1 The Fe^{16+} 3C/3D oscillator strength ratio

X-ray emission from Ne-like Fe^{16+} in the energy range between roughly 600 and 1200 eV has been observed in a variety of sources, like stellar coronae [3] or x-ray binaries [36]. Emission from Fe^{16+} offers diagnostics of plasma parameters over a wide range of temperatures and densities [37, 38]. The spectrum of this ion species has therefore been extensively studied [39]. Nevertheless, model spectra aren't accurate enough to exploit the full potential of high-resolution x-ray spectra recorded by satellite observatories. In particular, the $2p$–$3d$ resonance and intercombination lines at 826 eV (15.01 Å, $[(2p^5)_{1/2}\,3d_{3/2}]_{J=1} \rightarrow [2p^6]_{J=0}$, usually dubbed 3C) and 812 eV (15.26 Å, $[(2p^5)_{3/2}\,3d_{5/2}]_{J=1} \rightarrow [2p^6]_{J=0}$. usually dubbed 3D), respectively, have been at the center of extensive experimental and theoretical work, aimed at resolving a persistent disagreement of observations with predictions of their relative oscillator strengths.

A first resonant photoexcitation experiment on 3C and 3D was carried out with FLASH-EBIT at the LCLS free-electron laser, seemingly confirming the discrepancy, while hinting at inaccurate atomic structure calculations as a possible cause [30]. Since then, it has been pointed out that the high peak brilliance of LCLS might have introduced nonlinear excitation dynamics [40, 41] or nonequilibrium time evolution [42], which might have affected the fluorescence yields observed, and therefore the reported oscillator strength ratio. Furthermore, another transition ($[(2p^5)_{1/2}\,3s\,3d_{5/2}]_{J=3/2} \rightarrow [2p^6\,3s]_{J=1/2}$, usually dubbed C) in the neighboring charge state Fe^{15+} appeared blended with 3D, which could have led to a resonant population transfer between both ion species, which would also have manifested in a distortion of the apparent oscillator strength ratio [43].

Two experiments with PolarX-EBIT at beamline P04 of PETRA III have addressed these problems [44, 45]. Nonlinear effects were suppressed by an approximately six orders of magnitude lower peak brilliance compared to LCLS. The actual fluorescence photon count rates observed in the experiment were still of the same order, due to a much higher repetition rate of the photon pulses provided by the light source, combined with the larger solid angle for fluorescence detection offered by PolarX-EBIT. A more than ten times higher spectral resolution allowed for the first time to resolve the

2025 JINST 20 C03030

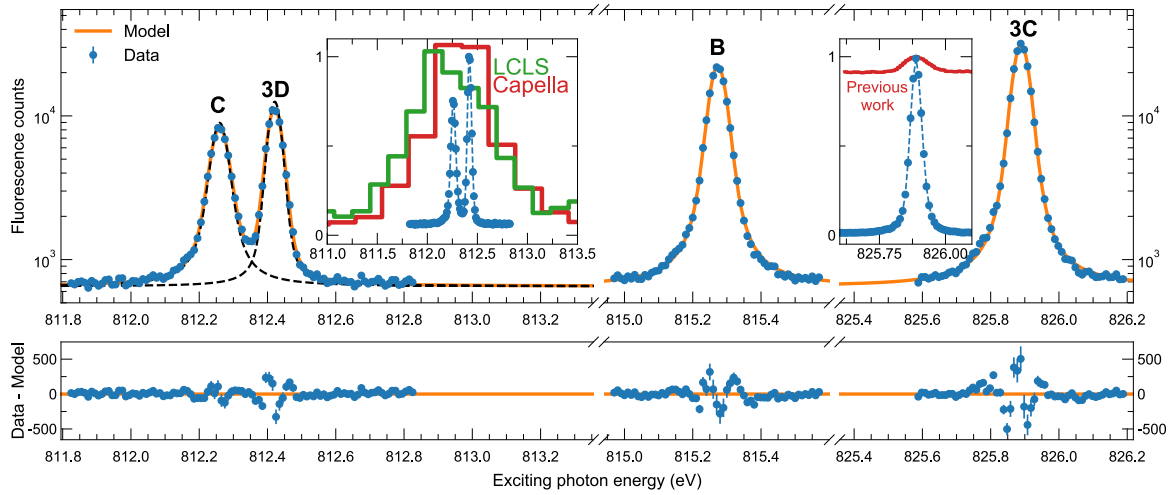

Figure 4. Fluorescence yields from iron ions in PolarX-EBIT recorded as functions of the exciting photons energy. Resonantly excited fluorescence from the soft x-ray transitions 3C and 3D of Fe^{16+}, as well as B and C of Fe^{15+}, is visible as peaks. Measured data are shown in blue, fitted Voigt profiles in orange. The inset on the left compares this measurement with a previous one at LCLS (green [30]) and observations of Capella with the Chandra X-ray Observatory (red [47]). The inset on the right illustrates the improved signal-to-noise ratio compared to the previous measurement at PETRA III (red [44]). Reproduced from [45]. CC BY 4.0.

blend between 3D and C, avoiding any potential population transfer. A comparison of the resolving power achieved during the LCLS measurement is shown in the left inset of figure 4. A key factor in achieving this increase in resolving power was the use of the monochromator at beamline P04 at the absolute limits of its technical capabilities. The count rates achieved for comparatively strong transitions in the ions studied allowed for repeated measuremnts and incremental optimization of beamline element and monochromator settings [46], as well as positioning of PolarX-EBIT.

While the first of both experiments seemed to confirm the LCLS result [44], an improved measurement scheme was introduced during the second. By rapidly switching between an electron beam energy sufficient for ion production and a lower one during recording of fluorescence, it was possible to remove a constant background signal caused by electron impact excitations and improve the signal-to-noise ratio thousandfold (see right inset of figure 4). This led to the uncovering of wide Lorentzian wings in the observed line shapes, that had hitherto not been included in oscillator strength determinations, due to being hidden in the background. After taking this effect into account, the experimental result of $f_{3C}/f_{3D} = 3.51(2)_{stat}(7)_{sys}$ is in agreement with newest calculations, predicting a value of 3.55(2) [45].

Additionally, the spectral resolution and signal-to-noise ratio achieved allowed to at least indirectly measure the natural linewidths of 3C and 3D. The values of 15.07(107) meV for 3C and 3.79(52) meV for 3D agree with theory within uncertainties. This is the first time that the individual transition rates of 3C and 3D, expressed in the form of linewidths, have been used to test atomic structure calculations, instead of the more accessible oscillator strength ratio.

Similar measurements were carried out on the lines 3C and 3D in Ni^{18+}, where a resolving power of 15,000 and a signal-to-noise ratio of 30 were achieved, resulting in the ability to obtain both natural linewidths with relative uncertainties below 10% [48]. The observed values are in good agreement with newest calculations.

2025 JINST 20 C03030

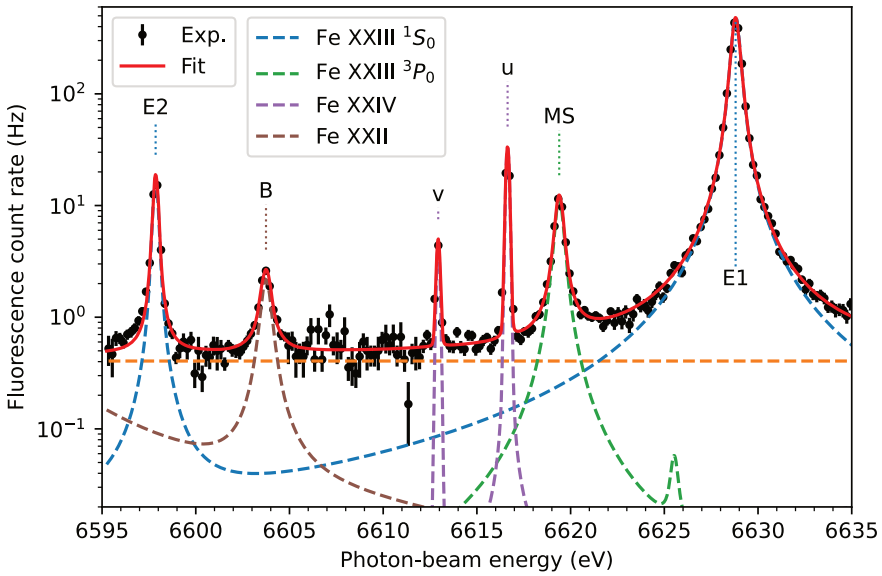

Figure 5. Resonantly excited fluorescence from iron ions in PolarX-EBIT at beamline P01 of PETRA III. The fluorescence yield is shown as a function of the energy of incoming photons. Data (black) are binned to 0.2 eV intervals for clarity. A fit of six Voigt profiles (red) is shown and models transitions from Li-like (u, v), Be-like (E1, E2, MS), and B-like (B) ions. The feature labeled MS originates from a transition out of an already excited metastable state. The dashed curves show contributions from the three charge states and a constant background to the model. Reproduced from [51]. The Author(s). CC BY 4.0.

3.2 Plasma density diagnostics with ions in metastable states

Ionized matter outflowing from AGN has been discussed to be a critical component of feedback between AGN and host galaxies [49]. Key parameters for understanding these outflows are mass and energy flow rates. Measuring them requires knowledge of local hydrogen-equivalent volume densities, for which local electron densities can serve as proxies. To measure them, it was proposed to use UV and x-ray absorption lines from ions in metastable states, because their populations compared to the respective ground states are sensitive to the electron density.

The electron beam in PolarX-EBIT can result in a significant population of ions in metastable states. Resonant absorption of x-ray photons by metastable Ne^{6+} was observed at beamline P04, and by metastable Fe^{20+} and Fe^{22+} at beamline P01 of PETRA III. An example spectrum is shown in figure 5. Resolving powers $E/\Delta E_{\mathrm{FWHM}}$ of 14,000 at 895 eV (P04) and 32,500 at 6.5 keV (P01) were achieved, sufficient to resolve the natural linewidths of multiple transitions. Using model state-population balances, calculated with the Flexible Atomic Code (FAC) [50], it was possible to determine metastable populations, and consequently the effective electron density in the electron beam of PolarX-EBIT [51]. This has successfully demonstrated the feasibility of density diagnostics based on these ions, which are commonly found in astrophysical plasmas, in observations with future high-resolution x-ray observatories.

3.3 Resonant photoionization

Photoionization plays an important role in the dynamics of many astrophysical plasmas [52], such as those in accretion disks around black holes. Resonant photoionization, i.e. resonant excitation

2025 JINST 20 C03030

by absorption of a photon followed by Auger decay, can lead to strong absorption lines and is a key process in plasma modeling. Experiments conducted with FLASH-EBIT at BESSY II and PETRA III have used the detection of ions extracted from the trap to measure resonant photoionization cross sections for multiple highly charged ion species [31, 32, 34].

PolarX-EBIT has been equipped with a beamline for time-of-flight measurements, which allows for measurements of charge state distributions of trapped ions. An electrostatic 90° bender and an electrostatic focusing lens are installed behind the collector. When the central trap electrode is switched from its trapping setting to a higher positive extraction voltage, using a high-voltage switch, ions are expelled from the trap and fly through collector, bender, and lens. The ion current is recorded by a channeltron detector as a function of time after switching.

This setup has been used at beamline P04 of PETRA III to measure resonant photoionization of Fe^{13+} into Fe^{14+}, detectable as a change of ion yield in both charge states while scanning the energy of incoming photons. In the energy range from 760 eV to 810 eV, multiple transitions of the so-called unresolved transition array (UTA) were observed, simultaneously in ion yield and fluorescence photons. This combined detection of autoionization and radiative relaxation gave access to the corresponding branching ratios.

3.4 Few-electron ions as x-ray energy references

Observations of the strong $1s-2p$ resonance line from atomic oxygen in the Milky Way surprisingly yielded a line position shifted compared to the laboratory value [53]. It matched a Doppler shift resulting from motion at a velocity of approximately 340 km/s. A value close to zero was expected. Literature values for atomic oxygen transitions have traditionally been measured using molecular oxygen (O_2) absorption spectra for calibration. These have been measured in the past using the electron energy loss spectroscopy (EELS) method [54, 55]. The x-ray observatories Chandra and XMM-Newton on the other hand have relied on H- and He-like HCI for calibration of their instruments. The apparent high-velocity motion of atomic oxygen in the Galaxy could be explained by a systematic shift between both calibration standards.

An experiment to investigate this possibility was carried out at beamline U49-2/PGM-1 of BESSY II [56]. PolarX-EBIT was installed after the plane-grating monochromator. An absorption cell with O_2 was installed downstream, utilizing the capabilities of the unique off-axis electron gun. The photon beam energy was scanned and fluorescence from $1s-np$ transitions of N^{5+} and O^{6+} in PolarX-EBIT was recorded. At the same time, a channeltron in the absorption cell recorded photoions produced by absorption in the gas. The newly measured O_2 absorption spectrum exhibits a shift compared to the original EELS measurements. Recalibrating the atomic oxygen observations with this new reference spectrum now excludes the previously suggested incongruent motion of interstellar oxygen. The same experimental setup was also used to measure and calibrate absorption spectra of Ne, CO_2, and SF_6 [57]. These spectra cover the energy range from 500 to 800 eV with accuracies better than 100 meV.

This demonstrated how electronic transitions in few-electron ions can serve as accurate and stable energy references for high-precision measurements at ultrabrilliant light sources. There is a need for reproducible x-ray energy calibration references at x-ray light sources, not only for atomic physics and astrophysics, but a growing number of users from different fields. Compared to absorption in gas cells or solid samples, highly charged ions are not susceptible to temperature or pressure changes, as well as chemical impurities. They are also largely insensitive to typical electric and magnetic

2025 JINST 20 C03030

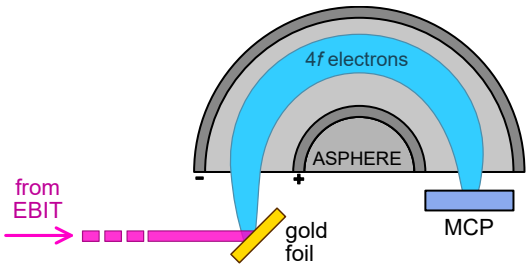

Figure 6. Setup of a photoelectron spectrometer for measuring changes in the energy of photons used for resonant-photoexcitation experiments with PolarX-EBIT. The photon beam is dumped onto a gold foil and resulting photoelectrons are guided through the ASPHERE electron spectrometer towards a position-sensitive micro-channel plate (MCP) detector. Changes in photon energy translate into changes in electron energy, which can be measured by compensating with a change of the voltage applied to the electrodes of the electron spectrometer.

fields found in laboratory environments. Narrow electronic transitions in highly charged ions are also available in large numbers over many orders of magnitude in energy.

Recently, a combination of PolarX-EBIT with the high-energy-resolution photoelectron spectrometer ASPHERE [58] has been used to track nonlinearities in the photon energy calibration of beamline P04, which led to further improvements in measurements, which now are reaching ppm-level accuracies and reproducibilities [59, 60]. This as achieved by exploiting the geometry of PolarX-EBIT, with its off-axis electron gun, which allows the photon beam to be transmitted through the trap and onto a gold foil (see figure 6). There, $4f$ photoelectrons are released into the ASPHERE electron spectrometer. After being guided through ASPHERE, they are imaged with a position sensitive detector. The voltage applied to the electron spectrometer determines the location where the electrons are detected. When changing the photon energy the kinetic energy of the photoelectrons leaving the gold foil changes by the same amount. Consequently, the electrons leave ASPHERE at a different location. The previous location can be restored by changing the voltage applied to the electron spectrometer. The required change in volts corrsponds directly to the actual change of photon energy in electronvolts. Therefore, the actual change of the energy of photons interacting with ions in PolarX-EBIT can be tracked from scan step to scan step. By establishing one or multiple absolute reference points, in the form of well-known transitions in few-electron ions, an absolute calibration of the photon energy axis for scans over wide energy ranges can by provided.

4 Conclusions and outlook

PolarX-EBIT has been used in multiple successful experimental campaigns at different ultrabrilliant synchrotron x-ray light sources. The technique of resonant photoexcitation has been used to measure transition energies, oscillator strengths, and branching ratios of importance for the interpretation of astrophysical x-ray spectra. Technical improvements have led to resolving powers and signal-to-noise ratios better by multiple orders of magnitude compared to state-of-the-art prior to development of PolarX-EBIT. This has enabled the detection of lower rate processes, like excitations from metastable states. Reduced uncertainties help benchmarking atomic structure calculations. Furthermore, processes like two-electron-one-photon transitions (TEOP) have been studied [61]. This also serves to benchmark parts of atomic structure theory, like electron-electron correlations.

2025 JINST 20 C03030

It has been demonstrated that electronic transitions in HCI can serve as reproducible x-ray energy calibration references for beamlines at light source facilities. Beyond that, PolarX-EBIT has been used to characterise and optimise x-ray optics [46]. For that purpose, narrow transitions in few-electron HCI were used as stable and known absorption features, allowing the reconstruction of apparatus profiles.

New EBITs based on the Heidelberg-compact-EBIT design have been built and are now in operation, including ones at PAL-XFEL, Spring8, and European XFEL. With multiple devices around the world operating at light sources covering a wide energy range, and also utilizing off-axis electron guns inspired by PolarX-EBIT, resonant photoexcitation measurements can be expected to contribute significantly to the repository of atomic data needed for modeling astrophysical plasmas and the interpretation of x-ray spectra recorded by high-resolution instruments onboard current and future satellite observatories. Beyond that, an EBIT nearly identical to PolarX-EBIT, the new SQS-EBIT at the European XFEL, is installed at a beamline offering two-color x-ray photon beams with precisely timed delays in the fs regime [62]. This opens up exciting new possibilities for x-ray pump-probe experiments on timescales relevant for electronic excitation dynamics in highly ionized plasmas. In contrast to these new EBITs, PolarX-EBIT is not settled at one radiation beamline, but designed to be relatively easy to transport and pioneer new experimental techniques at a wide variety of ultrabrilliant light sources.

Acknowledgments

Financial support was provided by the Max-Planck-Gesellschaft (MPG) and Bundesministerium für Bildung und Forschung (BMBF) through project 05K13SJ2. C. S. acknowledges support from MPG and NASA-JHU Cooperative Agreement. M. A. L. acknowledges support from NASA's Astrophysics Program. We acknowledge DESY (Hamburg, Germany), a member of the Helmholtz Association HGF, for the provision of experimental facilities. Parts of this research were carried out at PETRA III and we would like to thank the staff of beamlines P01 and P04 for their assistance. We thank HZB for the allocation of synchrotron radiation beamtime at BESSY II.

References

[1] C.R. Canizares et al., *The Chandra high energy transmission grating: Design, fabrication, ground calibration and five years in flight*, *Publ. Astron. Soc. Pac.* **117** (2005) 1144 [astro-ph/0507035].

[2] F.B.S. Paerels and S.M. Kahn, *High-resolution x-ray spectroscopy with chandra and xmm-newton*, *Ann. Rev. Astron. Astrophys.* **41** (2003) 291.

[3] E. Behar, J. Cottam and S.M. Kahn, *The Chandra iron-L x-ray line spectrum of Capella*, *Astrophys. J.* **548** (2001) 966 [astro-ph/0003099].

[4] J.R. Peterson et al., *High resolution x-ray spectroscopic constraints on cooling — flow models for clusters of galaxies*, *Astrophys. J.* **590** (2003) 207 [astro-ph/0210662].

[5] A.C. Fabian et al., *Hidden cooling flows in clusters of galaxies*, *Mon. Not. Roy. Astron. Soc.* **515** (2022) 3336 [arXiv:2207.04951].

[6] J.S. Kaastra et al., *X-ray absorption lines in the Seyfert 1 galaxy NGC 5548 discovered with Chandra-LETGS*, *Astron. Astrophys.* **354** (2000) L83 [astro-ph/0002345].

[7] S. Laha et al., *Ionized outflows from active galactic nuclei as the essential elements of feedback*, *Nature Astron.* **5** (2021) 13 [arXiv:2012.06945].

2025 JINST 20 C03030

[8] Y. Ezoe, T. Ohashi and K. Mitsuda, *High-resolution X-ray spectroscopy of astrophysical plasmas with X-ray microcalorimeters*, *Rev. Mod. Plasma Phys.* **5** (2021) 4.

[9] Hitomi collaboration, *The Quiescent Intracluster Medium in the Core of the Perseus Cluster*, *Nature* **535** (2016) 117 [arXiv:1607.04487].

[10] M.S. Tashiro, *XRISM: X-ray imaging and spectroscopy mission*, *Int. J. Mod. Phys. D* **31** (2022) 2230001.

[11] K. Nandra et al., *The Hot and Energetic Universe: A White Paper presenting the science theme motivating the Athena+ mission*, arXiv:1306.2307.

[12] Hitomi collaboration, *Atomic data and spectral modeling constraints from high-resolution X-ray observations of the Perseus cluster with Hitomi*, *Publ. Astron. Soc. Jap.* **70** (2018) 12 [arXiv:1712.05407].

[13] G. Betancourt-Martinez et al., *Unlocking the Capabilities of Future High-Resolution X-ray Spectroscopy Missions Through Laboratory Astrophysics*, arXiv:1903.08213.

[14] L. Gu et al., *X-ray spectra of the Fe-L complex*, *Astron. Astrophys.* **627** (2019) A51 [arXiv:1905.07871].

[15] P. Beiersdorfer, *Laboratory x-ray astrophysics*, *Ann. Rev. Astron. Astrophys.* **41** (2003) 343.

[16] T.R. Kallman and P. Palmeri, *Atomic Data for X-Ray Astrophysics*, *Rev. Mod. Phys.* **79** (2007) 79 [astro-ph/0610423].

[17] M.A. Levine et al., *The Electron Beam Ion Trap: A New Instrument for Atomic Physics Measurements*, *Phys. Scripta T* **22** (1988) 157.

[18] R.E. Marrs, P. Beiersdorfer and D. Schneider, *The Electron-Beam Ion Trap*, *Phys. Today* **47** (1994) 27.

[19] P. Beiersdorfer, *A "brief" history of spectroscopy on EBIT*, *Can. J. Phys.* **86** (2008) 1.

[20] K. Kubiček et al., *Transition energy measurements in hydrogenlike and heliumlike ions strongly supporting bound-state QED calculations*, *Phys. Rev. A* **90** (2014) 032508.

[21] C. Beilmann et al., *Major role of multielectronic K–L intershell resonant recombination processes in Li- to O-like ions of Ar, Fe, and Kr*, *Phys. Rev. A* **88** (2013) 062706.

[22] C. Beilmann, J.R.C. López-Urrutia, P.H. Mokler and J. Ullrich, *High resolution resonant recombination measurements using evaporative cooling technique*, 2010 *JINST* **5** C09002.

[23] P. Micke et al., *The Heidelberg compact electron beam ion traps*, *Rev. Sci. Instrum.* **89** (2018) 063109 [arXiv:2011.01363].

[24] C. Shah et al., *Laboratory measurements compellingly support charge-exchange mechanism for the 'dark matter' ~3.5 keV X-ray line*, *Astrophys. J.* **833** (2016) 52 [arXiv:1608.04751].

[25] A. Lapierre et al., *The TITAN EBIT charge breeder for mass measurements on highly charged short-lived isotopes — First online operation*, *Nucl. Instrum. Meth. A* **624** (2010) 54.

[26] T. Leopold et al., *A cryogenic radio-frequency ion trap for quantum logic spectroscopy of highly charged ions*, *Rev. Sci. Instrum.* **90** (2019) 073201.

[27] T.W. Hänsch and H. Walther, *Laser spectroscopy and quantum optics*, *Rev. Mod. Phys.* **71** (1999) S242.

[28] V. Mäckel et al., *Laser Spectroscopy on Forbidden Transitions in Trapped Highly Charged Ar^{13+} Ions*, *Phys. Rev. Lett.* **107** (2011) 143002.

[29] S.W. Epp et al., *X-ray laser spectroscopy of highly charged ions at FLASH*, *J. Phys. B* **43** (2010) 194008.

[30] S. Bernitt et al., *An unexpectedly low oscillator strength as the origin of the Fe xvii emission problem*, *Nature* **492** (2012) 225.

2025 JINST 20 C03030

[31] M.C. Simon et al., *Resonant and Near-Threshold Photoionization Cross Sections of Fe^{14+}*, Phys. Rev. Lett. **105** (2010) 183001.

[32] M.C. Simon et al., *Photoionization of N^{3+} and Ar^{8+} in an electron beam ion trap by synchrotron radiation*, J. Phys. B **43** (2010) 065003.

[33] J.K. Rudolph et al., *X-Ray Resonant Photoexcitation: Linewidths and Energies of K_α Transitions in Highly Charged Fe Ions*, Phys. Rev. Lett. **111** (2013) 103002.

[34] R. Steinbrügge et al., *Absolute measurement of radiative and Auger rates of K-shell-vacancy states in highly charged Fe ions*, Phys. Rev. A **91** (2015) 032502.

[35] S.W. Epp et al., *Single-photon excitation of K_α in heliumlike Kr^{34+}: Results supporting quantum electrodynamics predictions*, Phys. Rev. A **92** (2015) 020502.

[36] S.M. Kahn, F.D. Seward and T. Chlebowski, *High-resolution soft X-ray spectra of Scorpius X-1 — The structure of circumsource accreting material*, Astrophys. J. **283** (1984) 286.

[37] J.T. Schmelz, J.L.R. Saba and K.T. Strong, *Resonance scattering of Fe XVII — A density diagnostic*, Astrophys. J. **398** (1992) L115.

[38] G.V. Brown et al., *Diagnostic Utility of the Relative Intensity of 3C to 3D in Fe XVII*, Astrophys. J. **557** (2001) L75.

[39] C. Shah et al., *Revisiting the Fe XVII line emission problem: laboratory measurements of the 3s-2p and 3d-2p line-formation channels*, Astrophys. J. **881** (2019) 100 [arXiv:1903.04506].

[40] N.S. Oreshkina, S.M. Cavaletto, C.H. Keitel and Z. Harman, *Astrophysical Line Diagnosis Requires Nonlinear Dynamical Atomic Modeling*, Phys. Rev. Lett. **113** (2014) 143001.

[41] N.S. Oreshkina, S.M. Cavaletto, C.H. Keitel and Z. Harman, *X-ray fluorescence spectrum of highly charged Fe ions driven by strong free-electron-laser fields*, J. Phys. B **49** (2016) 094003.

[42] S.D. Loch et al., *Non-equilibrium modeling of the Fe XVII 3C/3D line ratio in an intense x-ray free-electron laser excited plasma*, Astrophys. J. **801** (2015) L13.

[43] C. Wu and X. Gao, *Change of the relative line strengths due to the resonance induced population transfer between Fe XVII and FeXVI ions*, Sci. Rep. **9** (2019) 7463.

[44] S. Kühn et al., *High Resolution Photoexcitation Measurements Exacerbate the Long-Standing Fe XVII Oscillator Strength Problem*, Phys. Rev. Lett. **124** (2020) 225001 [arXiv:1911.09707].

[45] S. Kühn et al., *New Measurement Resolves Key Astrophysical Fe XVII Oscillator Strength Problem*, Phys. Rev. Lett. **129** (2022) 245001 [arXiv:2201.09070].

[46] M. Hoesch et al., *Highly Charged Ions for High-Resolution Soft X-ray Grating Monochromator Optimisation*, J. Phys. Conf. Ser. **2380** (2022) 012086.

[47] D.P. Huenemoerder et al., *TGCat: The Transmission Grating Data Catalog and Archive*, Astron. J. **141** (2011) 129.

[48] C. Shah et al., *Natural-linewidth measurements of the 3C and 3D soft-x-ray transitions in Ni xix*, Phys. Rev. A **109** (2024) 063108 [arXiv:2404.14589].

[49] B. Husemann and C.M. Harrison, *Reality and myths of AGN feedback*, Nature Astron. **2** (2018) 196.

[50] M.F. Gu, *The flexible atomic code*, Can. J. Phys. **86** (2008) 675.

[51] R. Steinbrügge et al., *X-Ray Photoabsorption of Density-sensitive Metastable States in Ne vii, Fe xxii, and Fe xxiii*, Astrophys. J. **941** (2022) 188.

2025 JINST 20 C03030

[52] R.C. Mancini et al., *Accretion disk dynamics, photoionized plasmas, and stellar opacities*, *Phys. Plasmas* **16** (2009) 041001.

[53] T.W. Gorczyca et al., *A comprehensive x-ray absorption model for atomic oxygen*, *Astrophys. J.* **779** (2013) 78.

[54] G.R. Wight and C.E. Brion, *K-shell excitations in NO and O_2 by 2.5 keV electron impact*, *J. Electron Spectrosc. Rel. Phenom.* **4** (1974) 313.

[55] A.P. Hitchcock and C.E. Brion, *K-shell excitation spectra of CO, N2 and O2*, *J. Electron Spectrosc. Rel. Phenom.* **18** (1980) 1.

[56] M. Leuteneggercet al., *High-Precision Determination of Oxygen K_α Transition Energy Excludes Incongruent Motion of Interstellar Oxygen*, *Phys. Rev. Lett.* **125** (2020) 243001.

[57] J. Stierhof et al., *A new benchmark of soft X-ray transition energies of Ne, CO_2, and SF_6: paving a pathway towards ppm accuracy*, *Eur. Phys. J. D* **76** (2022) 38.

[58] K. Rossnagel, L. Kipp, M. Skibowski and S. Harm, *A high performance angle-resolving electron spectrometer*, *Nucl. Instrum. Meth. A* **467–468** (2001) 1485.

[59] C. Shah et al., *High-precision Transition Energy Measurements of Neon-like Fe XVII Ions*, *Astrophys. J.* **969** (2024) 52 [arXiv:2401.08395].

[60] M. Togawa et al., *High-accuracy measurements of core-excited transitions in light Li-like ions*, *Phys. Rev. A* **110** (2024) L030802.

[61] M. Togawa et al., *Observation of strong two-electron–one-photon transitions in few-electron ions*, *Phys. Rev. A* **102** (2020) 052831 [arXiv:2003.05965].

[62] S. Serkez et al., *Opportunities for Two-Color Experiments in the Soft X-ray Regime at the European XFEL*, *Appl. Sci.* **10** (2020) 2728.

2025 JINST 20 C03030